Pathol. Oncol. Res. (2018) 24:515–524
DOI 10.1007/s12253-017-0262-y

ORIGINAL ARTICLE

Distribution of Vascular Patterns in Different Subtypes of Renal Cell Carcinoma. A Morphometric Study in Two Distinct Types of Blood Vessels

Amparo Ruiz-Saurí[1,2] · V. García-Bustos[1] · E. Granero[1] · S. Cuesta[1] · M. A. Sales[3] · V. Marcos[1] · A. Llombart-Bosch[1]

Received: 18 November 2016 / Accepted: 21 June 2017 / Published online: 1 July 2017

Abstract To analyze the presence of mature and immature vessels as a prognostic factor in patients with renal cell carcinoma and propose a classification of renal cancer tumor blood vessels according to morphometric parameters. Tissue samples were obtained from 121 renal cell carcinoma patients who underwent radical nephrectomy. Staining with CD31 and CD34 was used to differentiate between immature (CD31+) and mature (CD34+) blood vessels. We quantified the microvascular density, microvascular area and different morphometric parameters: maximum diameter, minimum diameter, major axis, minor axis, perimeter, radius ratio and roundness. We found that the microvascular density was higher in CD31+ than CD34+ vessels, but CD34+ vessels were larger than CD31+ vessels, as well as being strongly correlated with the ISUP tumor grade. We also identified four vascular patterns: pseudoacinar, fascicular, reticular and diffuse. Pseudoacinar and fascicular patterns were more frequent in clear cell renal cell carcinoma (37.62 and 35.64% respectively), followed by reticular pattern (21.78%), while in chromophobe tumors the reticular pattern predominated (90%). The isolated pattern was present in all papillary tumors (100%). In healthy renal tissue, the pseudoacinar and isolated patterns were differentially found in the renal cortex and medulla respectively. We defined four distinct vascular patterns significantly related with the ISUP tumor grade in renal cell carcinomas. Further studies in larger series are needed in order to validate these results. Analysis of both mature and immature vessels (CD34+ and CD31+) provides additional information when evaluating microvascular density.

Keywords Clear cell renal cell carcinoma · Papillary renal cell carcinoma · Chromophobe renal cell carcinoma · Microvascular density · Microvascular area · Morphometry · CD31 · CD34 · Renal vascular patterns

Introduction

Renal Cell Carcinoma (RCC) has a significant place among studies of angiogenesis due to its high incidence rate and dense vascularity. The formation of new vessels is a decisive factor in the process of tumor growth, providing nutrients to the tumor tissue and oxygen necessary for their proliferation [1]. It has been established that tumor vascularization does not exclusively derive from the proliferation of endothelial cells, but also involves other complex factors and mechanisms leading to the formation of a vascular network which allows tumor growth [2]. This complexity might be the reason for the lack of accurate procedures in the evaluation of blood neovessel morphology and phenotype in renal tumors.

The main categories of kidney tumors are Clear Cell Renal Cell Carcinoma (CCRCC), Papillary Carcinoma (PRCC) and Chromophobe Renal Cell Carcinoma (ChrRCC). The CCRCC type is the most common histological subtype and accounts for 60–70% of all RCCs. Although it may occur in all age groups, it most commonly affects patients in the sixth to seventh decades of life, the majority are males with a ratio of approximately 2:1 [3]. Microscopically tumor cells are arranged in compact nests, sheets, alveolar, or acinar structures

✉ Amparo Ruiz-Saurí
Amparo.Ruiz-Sauri@uv.es

[1] Department of Pathology, Faculty of Medicine and Odontology, University of Valencia, Avda. Blasco Ibañez n° 15, CP, 46010 Valencia, Spain

[2] INCLIVA, Biomedical Research Institute, Valencia, Spain

[3] Department of Pathology, University Clinical Hospital, Valencia, Spain

separated by thin-walled blood vessels. They have clear cytoplasm due to loss of cytoplasmic lipid and glycogen during tissue processing and slide preparation. In high-grade and poorly-differentiated tumors, cells acquire granular eosinophilic cytoplasm [4].

PRCC is the second most common type of RCC and accounts for 10–15% of RCCs. The gender and age distribution are similar to those of CCRCC [3]. Microscopically, PRCC is composed of varying proportions of papillae, tubulopapillae, and tubules. Two subtypes of PRCC are recognized based on the histology [5]. Accounting for about two- thirds of PRCC, type I tumor contains papillae that are delicate and short, lined with a single layer of tumor cells with scant cytoplasm and low-grade nuclei. In contrast, papillae in type II PRCC are large and lined with cells having abundant eosinophilic cytoplasm and large pseudostratified nuclei with prominent nucleoli. Patients with type I PRCC have a better prognosis than those with type II tumor [5].

ChrRCC accounts for approximately 5% of RCCs and is believed to arise from the intercalated cells of the collecting ducts [6]. ChrRCC can occur in a wide age range of patients. Males and females are affected almost equally. The prognosis is significantly better than for CCRCC, with disease recurrence in <5% of patients [3]. Microscopically, the tumor cells are usually arranged in solid sheets with some cases demonstrating areas of tubulocystic architecture. The classic ChrRCC tumor consists of large and polygonal cells with finely reticulated cytoplasm due to numerous cytoplasmic microvesicles, and prominent "plant cell like" cell membrane. The nuclei are typically irregular, hyperchromatic and wrinkled with perinuclear haloes. An eosinophilic variant, consisting predominantly of cells with intensely eosinophilic cytoplasm is not infrequent [7].

Microvascular density (MVD) is currently used to estimate microvasculature in many tumors, despite substantial limitations, due mainly to the complex biology of the tumor microvasculature [8] and the irregular geometry the microvascular system assumes in real space [9]. MVD is expressed as the number of microvessels per square millimeter in the subjectively-selected most vascularized area of tumor tissue (hot spots) [10]. However, this estimation does not achieve the resolution required to describe the two-dimensional geometrical complexity of the microvascular system, which mainly depends on: 1: the number of vessels; 2: the variability in vessel shapes and magnitudes; and 3: the pattern of vessel distribution [11].

Data on the mechanisms and significance of microvascular density in renal carcinoma are limited, despite the large number of papers that have been published. Furthermore, little evidence has been published about the development of tumor vascularization from the objective point of view of morphometry. The aim of this study was to analyze the presence of immature and mature vessels as a prognostic factor in patients with renal cell carcinoma and propose a classification of renal cancer tumor blood vessels according to their morphology and morphometric parameters.

Materials and Methods

Selection of Cases

The study protocol was reviewed and approved by the appropriate institutional ethics committees. Formalin fixed and paraffin-embedded specimens were collected from 121 patients with histopathologically verified CCRCC [12] who underwent nephrectomy between 1998 and 2011 at the Hospital Clínico Universitario of Valencia. All patients were treated with surgery alone. Histological diagnosis was based on hematoxylin-eosin staining by two senior pathologists experienced in RCC diagnosis. Tumors were staged according to the 6th AJCC TNM staging system and graded according to ISUP nucleolar grading system [13, 14]. Normal control tissue samples were obtained from non-tumor areas of the cortical region of the kidneys. Survival data were available for all 121 patients.

Immunohistochemistry

The immunohistochemical protocol was carried out by means of previously standardized DAKO Autostainer system. Mouse monoclonal antibodies against human CD31 and CD34 were used (clones JC70A and QBEnd respectively, DAKO, Glostrup, Denmark). Antigen retrieval was performed by autoclaved incubation for 3 min at 1.5 atm with citrate buffer pH 6.1. The sections were then washed three times with Tris buffered Saline (TBS). The peroxidase activity was visualized using 3.3 diaminobenzidine (DAB) and imidazole (0.01) as chromogen. CD31 was counterstained with hematoxylin-eosin.

Quantification by Morphometry

Microscopic evaluation and micrograph caption was performed with the optical microscope Leica DMD108 (Leica Microsystems S.L.U, Barcelona, Spain), under several magnifications: 40×, 100×, 200×, 400× and 630×.

For angiogenesis quantification, the samples were firstly visualized under lower magnifications (40× and 100×), which identifies the tumor areas and marks the "hot spots": the tumor area with the highest density of blood vessels. Then, six 200× magnification microphotographs of contiguous areas were taken in each sample, avoiding necrosis, inflammatory infiltrates and hemorrhage, resulting in a total 726 images for each of the CD31 and CD34 immunohistochemical stainings for our 121 cases. In the control cases, 6 micrographs of normal organized renal tissue showing elevated vascularization were

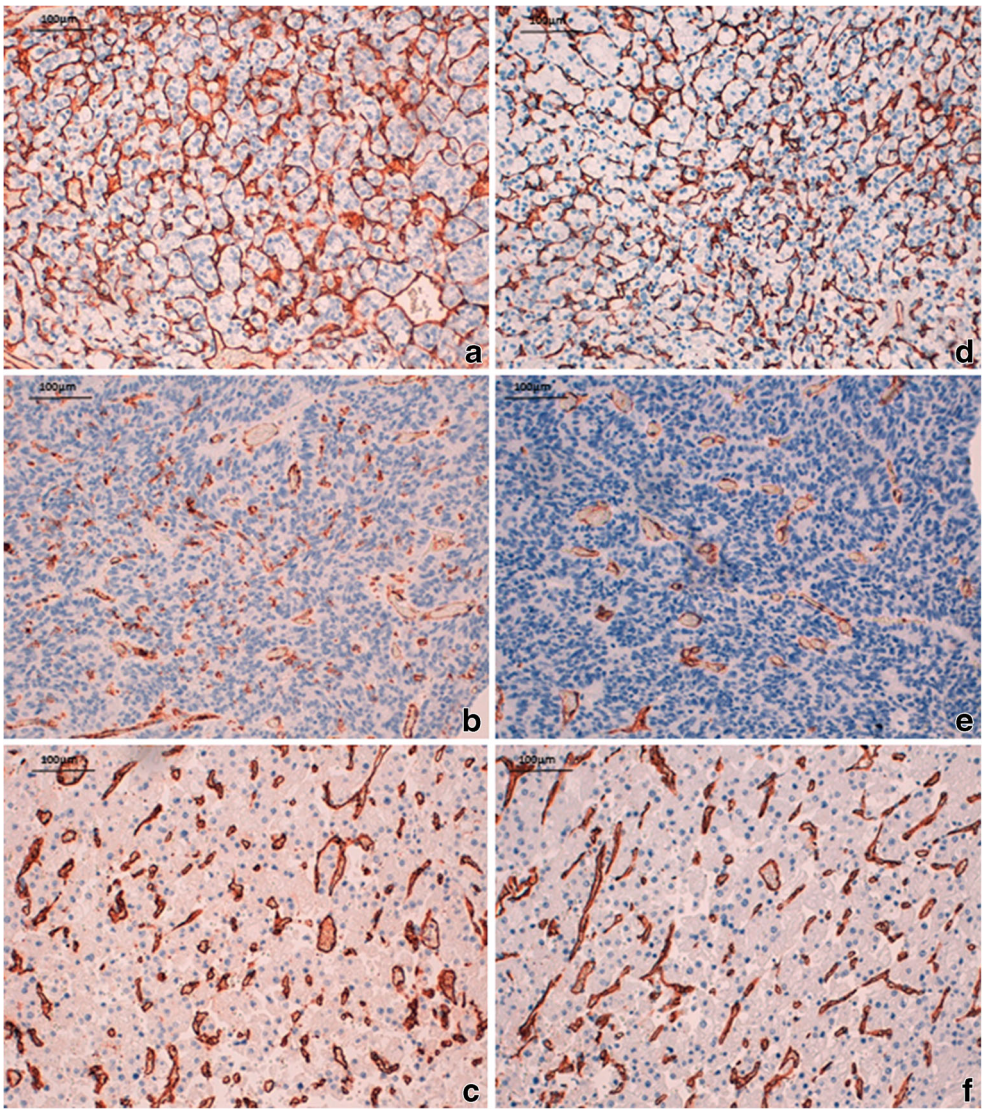

Fig. 1 Differential immunostaining comparing CD31+ and CD34+ blood vessels. 200× magnification. CD31+ vessels, 200× magnification: **a** Clear Cell Renal Cell Carcinoma; **b** Papillary Renal Cell Carcinoma; **c** Chromophobe Renal Cell Carcinoma. CD43+ vessels, 200× magnification: **d** Clear Cell Renal Cell Carcinoma; **e** Papillary Renal Cell Carcinoma; **f** Chromophobe Renal Cell Carcinoma

Table 1 Comparative analysis of variables according to the histological subtype of RCC for the marker CD31

	Healthy Kidney (mean ± SD)	Clear Cells (mean ± SD)	Papillary (mean ± SD)	Chromophobe (mean ± SD)
MVD	298.95 ± 27.41	923.96 ± 493.03	186.56 ± 67.15	241.62 ± 124.69
MVA	244.94 ± 50.40	92.02 ± 45.07	160.78 ± 76.16	312.75 ± 77.22
Major axis	29.15 ± 3.87	13.39 ± 8.38	20.68 ± 6.01	34.04 ± 5.19
Minor axis	12.12 ± 1.78	5.72 ± 2.99	8.66 ± 2.31	12.12 ± 2.16
R. Axis	0.42 ± 0.04	0.41 ± 0.03	0.42 ± 0.05	0.36 ± 0.04
Dm max	29.87 ± 3.99	15.82 ± 3,55	21.13 ± 6.42	34.91 ± 5.76
Dm min	8.66 ± 0.46	3.96 ± 0,71	7.03 ± 1.76	9.70 ± 1.66
R. Dm	0.30 ± 0.04	0.36 ± 0.04	0.34 ± 0.04	0.28 ± 0.04
Perimeter	87.80 ± 15.15	43.70 ± 15.66	62.00 ± 20.53	99.43 ± 20.20
Radius ratio	12.32 ± 3.19	11.56 ± 3.74	8.45 ± 2.58	11.73 ± 3.20
Roundness	2.92 ± 0.69	2.42 ± 0.40	2.23 ± 0.54	2.71 ± 0.52

MVD microvascular density in vessels/mm^2, *MVA* microvascular area in number of vessels/µm^2 of tissue, *R. Axes* relation between the axes (value of the minor axis/value of the major axis), *Dm max* Maximum diameter in µm, *Dm min* minimum diameter in µm, *R. Dm* relation between the diameters (value of the minimum diameter/value of the maximum diameter), *SD* standard deviation

Table 2 Comparative analysis of variables according to the histological subtype of RCC for the marker CD34

	Healthy Kidney (mean ± SD)	Clear Cells (mean ± SD)	Papillary (mean ± SD)	Chromophobe (mean ± SD)
MVD	393.23 ± 45.85	762.54 ± 412.54	156.16 ± 69.55	229.42 ± 140.59
MVA	1032.04 ± 643.76	208.34 ± 83.46	165.77 ± 58.31	1815.13 ± 1639.40
Major axis	50.97 ± 18.95	17.83 ± 12.05	22.50 ± 4.44	100.03 ± 128.52
Minor axis	21.36 ± 7.29	7.29 ± 5.18	9.21 ± 1.68	34.38 ± 40.99
R. Axis	0.42 ± 0.02	0.42 ± 0.04	0.41 ± 0.04	0.36 ± 0.04
Dm max	52.77 ± 19.25	17.07 ± 3.77	23.07 ± 4.88	103.74 ± 136.53
Dm min	16.63 ± 5.76	4.33 ± 0.62	7.51 ± 1.10	27.56 ± 34.09
R. Dm	0.30 ± 0.03	0.26 ± 0.04	0.33 ± 0.04	0.28 ± 0.04
Perimeter	160.38 ± 57.89	65.66 ± 12.22	67.08 ± 17.51	299.00 ± 398.70
Radius ratio	9.37 ± 2.15	12.70 ± 3.02	7.87 ± 2.23	18.87 ± 27.82
Roundness	2.70 ± 0.24	2.84 ± 0.64	2.47 ± 0.48	6.33 ± 11.55

MVD microvascular density in vessels/mm^2 , *MVA* microvascular area in number of vessels/μm2 of tissue, *R. Axes* relation between the axes (value of the minor axis/value of the major axis), *Dm max* Maximum diameter in μm, *Dm min* minimum diameter in μm, *R. Dm* relation between the diameters (value of the minimum diameter/value of the maximum diameter), *SD* standard deviation

also performed. Finally, these images were analyzed in order to obtain morphometric parameters with biomedical image analysis software Image-Pro Plus 7.0 (Infaimon, Media Cybernetics) in a semi-automatized manner.

The morphometric parameters selected for the evaluation of angiogenesis were:

- Total count: total number of selected objects in the microphotograph. This variable corresponds to the total number of vessels which, divided by 0.32 (total field area in mm^2 under 200× magnification), provides the variable of microvascular density (MVD), or number of vessels per square micrometer of tissue.
- Microvascular area (MVA): mean area of each blood vessel in μm^2 regardless of vessel lumen.
- Maximum diameter: length in μm of the longest straight line connecting two points of the contour of the vessel traversing its center.

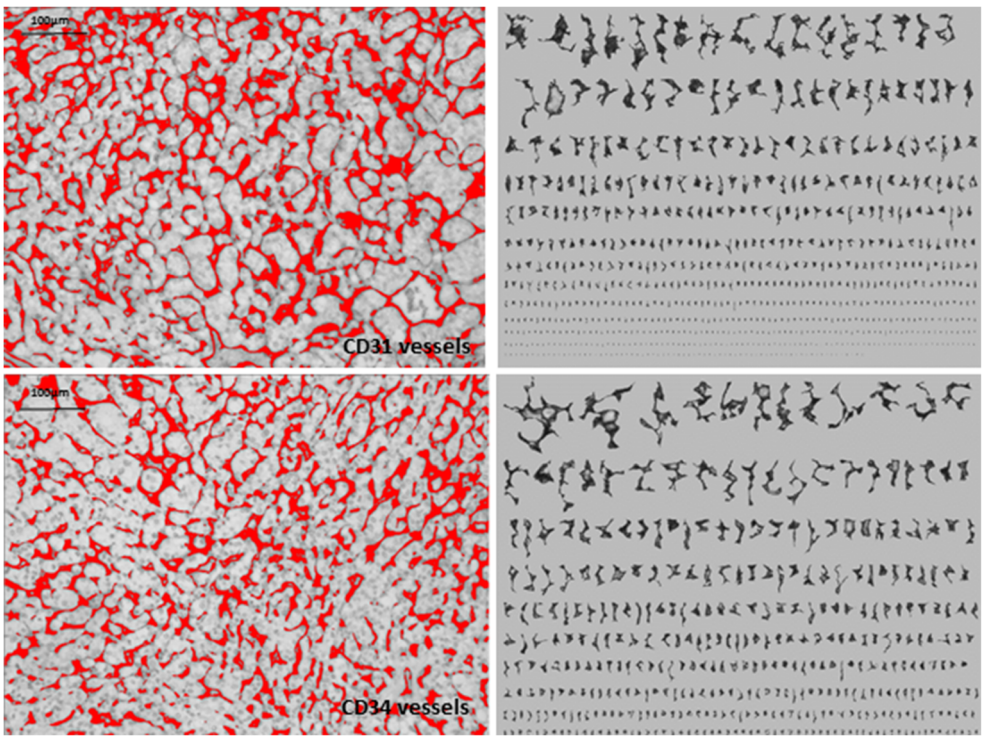

Fig. 2 Segmentation of CD31+ and CD34+ vessels. Images on the right show all the vessels organized by size. Notice the higher amount of CD31+ vessels and their smaller size

Table 3 Mean of MVA in CCRCC in CD31+ and CD34 + vessels according to ISUP tumor grading system

Number of cases	G-1 7	G-2 37	G-3 42	G-4 15
Mean MVA CD31 ± SD	108.95 ± 89.91	98.32 ± 76.76	84.56 ± 76.76	89.41 ± 88.07
Mean MVA CD34 ± SD	358.87 ± 623.27	163.28 ± 212.97	238.45 ± 435.71	164.90 ± 76.72

- Minimum diameter: length in μm of the shortest straight line connecting two points of the contour of the vessel traversing its center.
- Major axis: length in μm of the major axis of the ellipse equivalent to the vessel (this is the ellipse with the same area and angular momentum as the vessel).
- Minor axis: length in μm of the minor axis of the ellipse equivalent to the vessel
- Perimeter: length in μm of the line along the contour of each vessel.
- Radius ratio: ratio between the maximum radius of the vessel and the minimum radius thereof.
- Roundness: gives a numerical indication how round a vessel is. 1 refers to a perfectly circular object whilst other forms would be higher than unity. It is calculated with the following formula:

$$Roundness = perimeter^2 \Big/ 4\pi \text{ x } area$$

In addition, from the parameters obtained, the axial (value of the minor axis/value of the major axis) and diameter (value of the minor diameter/value of the major diameter) ratios were calculated. Using the data of axial ratio and vessel morphology we developed an objective morphological criterion in order to classify each tumor according to a vascular pattern. We set the cut point between 0.18 and 0.43, defining:

- Pseudoacinar pattern: High axial ratio (0.41–0.43). Round vessels, with a distinct and narrow lumen. They appear surrounding small tumor masses, resembling an acinar structure.
- Fascicular pattern: Low axial ratio (0.18–0.38). The major axis is higher than the minor axis. Hence, the vessels are elongated, interconnected and their lumen is very narrow or even collapsed.
- Reticular pattern: Widespread axial ratio (0.32–0.40), indicating that both round vessels with narrow but evident lumen and elongated vessels with collapsed lumen vessels are found. They appear ramified and anastomose creating a reticle.
- Isolated pattern: Intermediate axial ratio (0.39–0.41). The vessels are either round or elongated but short, with visible lumen, localized among tumor cells without evident interconnections.

Statistical Analysis

The statistical analysis of the obtained parameters was carried out using SPSS 17.0 for Windows 7 (SPPS Inc., Chicago, United States). The level considered to indicate statistical significance was $p < 0.05$.

The descriptive statistics for each morphometric parameter were calculated and the Kolmogorov-Smirnov normality test was performed for each sample. The appropriate statistical tests for hypothesis contrasts were used according to the characteristics of the samples, data and the number of groups to compare.

Results

Two distinct types of microvessels can be identified in CCRCC. CD34 immunostaining marks differentiated endothelial cells and CD31 immunostaining marks both differentiated and undifferentiated cells [15]. We studied the MVD and different morphometric parameters in vessels stained with CD31 and in vessels stained with CD34 in 121 RCC. 101 out of 121 cases (80.15%) were CCRCC, 10 cases (8.26%) were PRCC and 10 cases (8.26%) were ChrRCC. In addition, we studied five samples of healthy renal tissue which served as a control group. In all RCC samples we have demonstrated that the $CD31^+$ MVD was higher than $CD34^+$ MVD, being statistically significant in CCRCC ($p < 0.0001$). Figure 1 presents a comparative scheme between $CD31^+$ vessels and $CD34^+$ vessels in the three types of tumors.

Table 4 Mean of MVD in CCRCC in CD31+ and CD34 + vessels according to ISUP tumor grading system

Number of cases	G-1 7	G-2 37	G-3 42	G-4 15
Mean MVD CD31 ± SD	1104.38 ± 455.70	974.60 ± 445.96	887.44 ± 506.02	817.08 ± 588.82
Mean MVD CD34 ± SD	1147.84 ± 466.79	879.47 ± 375.58	661.17 ± 363.14	578.12 ± 443.79

Table 5 Mean of MVA in CCRCC in CD31+ and CD34 + vessels according to pT stage of the TNM staging system

Number of cases	pT1 15	pT2 34	pT3 49	pT4 3
Mean MVA CD31 ± SD	140.14 ± 130.66	81.16 ± 70.05	85.95 ± 82.63	73.29 ± 52.28
Mean MVA CD34 ± SD	396.30 ± 706.43	153.35 ± 207.10	191.32 ± 252.18	169.61 ± 348.28

When comparing both immunostainings, it was found that the MVA was higher in $CD34^+$ than $CD31^+$ vessels, however this difference is only statistically significant in CCRCC and ChrRCC ($p < 0.05$ and $p < 0.018$ respectively). See Tables 1 and 2. Moreover, $CD31^+$ vessels usually present smaller lumens, thicker walls and smaller areas compared with $CD34^+$ vessels, which are larger and with wider lumens. In Fig. 2 we present an image of the vessel segmentation procedure as well as a view of all CD31+ and CD34+ vessels in a sample, organized by area and shape.

Besides MVD and MVA, the other morphometric parameters were also compared in the $CD31^+$ and $CD34^+$ vessels. When examining the total 121 cases, the mean value for each of the different morphometric parameters was higher in $CD34^+$ vessels than in $CD31^+$ vessels, except R. Dm which was higher in CD31 vessels in CCRCC and PPRCC and equal in ChrRCC. The R. Axis was always higher in CD31 vessels in PPRCC; however, these differences were not statistically significant. See Tables 1 and 2.

In Tables 1, 2, 3, 4, 5 and 6 we indicate the number of cases, the mean MVA and the mean MVD of CCRCC by tumor T stage and ISUP tumor grade in both immunostainings. We found a declining trend in all cases which inversely correlates with T stage and ISUP grade, although these differences were only significant in the MVD of $CD34^+$ vessels in G1-G3/G4 comparisons ($p < 0.05$).

Immunostaining (CD31 and CD34) of the three tumor categories reveals that MVD increases significantly in CCRCC compared to PRCC and ChrRCC ($p < 0.0001$), as well as healthy renal tissue ($p < 0.05$). However, the MVA is significantly higher in ChrRCC compared to CCRCC and PRCC ($p < 0.05$).

Lastly, we established four histological blood vessel distribution patterns derived from the objective morphometric parameters resulting from the axial ratio as well as the subjective morphological features of the vessels. See Table 7 and Fig. 3. Pseudoacinar and fascicular patterns were more frequent in clear cell renal cell carcinoma (37.62 and 35.64% respectively), followed by the reticular pattern (21.78%). In chromophobe tumors the reticular pattern predominated (90%). The isolated pattern was present in practically all papillary tumors (90%). These differences were statistically significant ($p \leq 0.005$). In our controls, the pseudoacinar pattern predominated. In this last pattern, vessels were smaller, with intermediate to high MVD, and related with low T stages. In the fascicular pattern, blood vessels were small as well, but presented with high MVD, being associated with high T stages. In the reticular pattern, the vessels were larger; however the MVD was low and related to intermediate T stages. The isolated pattern followed the same trend as the reticular, but significantly related to low T stages. See Tables 8, 9 and Fig. 1.

Discussion

Although much remains unknown about the mechanisms of angiogenesis [16], MVD has been shown to predict prognosis for various malignant tumors, including lung cancer [17], breast cancer [18], and colorectal cancer [19]. However, whether MVD can predict prognosis in patients with RCC is controversial. In this regard, our team has previously demonstrated that increased angiogenesis is related to poorer prognosis [20] in agreement with other authors [21–25]. Nevertheless, many retrospective studies have reported MVD to be inversely related to survival in RCC [26–30]. Furthermore, a third group of researchers [24, 31] claims that no such relationship between MVD and prognosis exists. The inconsistency between these different findings suggests that MVD alone is not reliably associated with survival of patients with RCC. These discrepancies reflect the need to take into account the microvasculature differentiation as well as the morphometric parameters (Table 10).

We studied the vascularization of a new series of renal tumors and, despite using the same procedures as previous studies on angiogenesis, our results demonstrate an inverse relation between the number of vessels and the prognosis of these tumors. We found that vessels with higher $CD34^+$ significantly

Table 6 Mean of MVD in CCRCC in CD31+ and CD34 + vessels according to pT stage of the TNM staging system

Number of cases	pT1 15	pT2 34	pT3 49	pT4 3
Mean MVD CD31 ± SD	829.89 ± 427.71	971.87 ± 483.61	930.41 ± 521.19	745.83 ± 584.00
Mean MVD CD34 ± SD	846.35 ± 312.16	839.21 ± 419.30	676.66 ± 407.97	745.83 ± 584.00

Table 7 Distribution of the vascularization pattern according to tumor and vessel types

	Pseudoacinar	Fascicular	Reticular	Isolated
CD31				
CCRCC	39	35	27	-
PRCC	1	-	-	9
ChrRCC	1	-	9	-
CD34				
CCRCC	48	27	22	
PRCC	2	-	-	8
ChrRCC	2	-	8	

related to lower ISUP grade tumors ($p < 0.001$). This suggests that the architecture of vessels in renal carcinoma is different from that found in other types of malignancies [32]. Architectural differences are seen not only between tumors, but also between different regions of the same tumor. MVD [33, 34] and VEGF expression [35] are the two most frequently studied topics with respect to vasculature in renal cell carcinomas and to a lesser extent with other growth factors [36, 37].

This controversy led our team to study the vascular architecture of this tumor from an additional perspective to MVD alone. Using objective morphometric parameters we depicted the architectural pattern of neovessels in three histological varieties of renal tumors. These are: maximum diameter, minimum diameter, major axis, minor axis, perimeter, radius ratio, and blood vessel roundness. Despite the lack of statistically significant differences in the variables, these morphometric parameters allowed us to observe particular patterns of vascular organization in each type, with demonstrated significant correlations with histopathological data and tumor grade.

Description of patterns upon which the study was based:

The pseudoacinar pattern is formed by both round and elongated vessels with manifest lumens which, occasionally, may be narrowed or even collapsed. Capillary interconnections are abundant and arranged around small tumor masses mimicking an acinar or glomerular structure. It is fundamentally found in the CCRCC and is associated with low tumor grades.

The fascicular pattern presents clearly elongated vessels with either narrow or collapsed lumens, which branch widely to interconnect with each other. In CCRCC, this pattern is related to higher tumor grades.

In the reticular pattern, the vessels are generally elongated, their lumens are narrow or collapsed and branch and anastomose creating a reticle. This pattern is associated with intermediate tumor grade and is typical of ChrRCC.

The isolated pattern has short round and elongated vessels, with visible lumens, found among tumor cells but

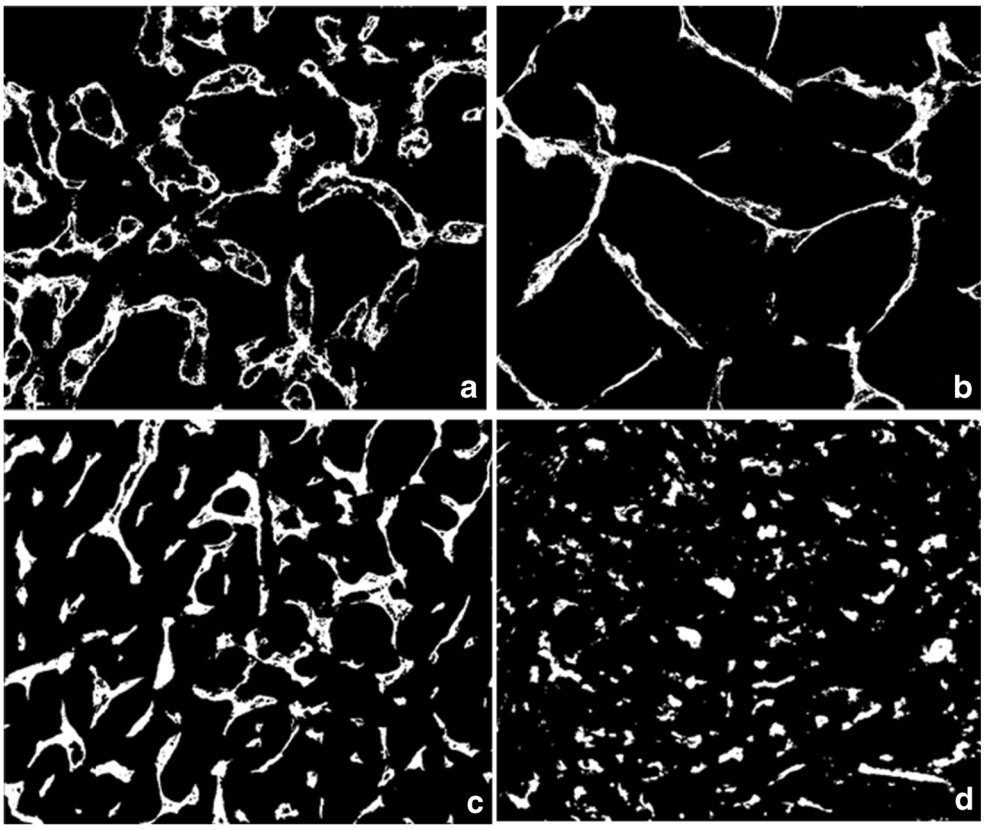

Fig. 3 Representative mask of the different vascular patterns of renal tumors. **a** pseudoacinar (Clear Cell Renal Cell Carcinoma; **b** Segmented (Clear Cell Renal Cell Carcinoma); **c** Reticular (Chromophobe Renal Cell Carcinoma); **d** scattered (Papillary Renal Cell Carcinoma)

Table 8 MVA and MVD according to vascularization patterns

MVA	Pseudoacinar	Fascicular	Reticular	Isolated
Small	27	28	10	3
Intermediate	18	4	18	5
Large	4	3	9	1
MVD				
Low	2	10	17	10
Intermediate	18	13	17	-
High	18	11	3	-

showing no interconnections. This pattern is related with low tumor grade and is mainly found in PRCC.

The different tumors do not present a unique vascular pattern but instead a high vascular heterogeneity, especially the CCRCC. The different combination of these depicted patterns could explain the large disparity reported regarding the prognostic value of MVD.

CCRCC with predominate pseudoacinar pattern is related with high MVD but low TNM grades, and shows a better prognosis. On the other hand, if the fascicular pattern is predominant in this type of tumor, the MVD would also be increased and would be associated with increased TNM stages. This strongly suggests that vessel morphology directly influences the release of pro and/or antiangiogenic factors, the vessel phenotype having a specific relation with tumor cells which would either promote or slow the growth of the tumor mass. Moreover, the microenvironment of solid human tumors is characterized by heterogeneity in oxygenation. Those tumors presenting vessels with elongated shapes and collapsed lumens, that is with a predominantly fascicular pattern, would receive less oxygen. The proliferation of a network of blood vessels with manifest lumen penetrating into the tumor mass would easily supply oxygen and nutrients and remove waste products. Tumors with low oxygenation have poorer prognosis, and strong evidence suggests that this is due to the effects of hypoxia on malignant progression, angiogenesis, metastasis, and resistance to therapy [38]. All this suggests that the special characteristics of the vascular network, depending on the vessel wall thickness, the integrity of the basal membrane of endothelial cells, the connections between the cells as well as the vessel distribution, would decisively influence tumor mass proliferation.

Table 9 Relation of vascular pattern with ISUP tumor grade in CCRCC

	Pseudoacinar	Fascicular	Reticular	Isolated
CCRCC				
Grades I and II	39		5	
Grades III and IV		30	27	

Table 10 Relation of vascular pattern with stage T in CCRCC, PRCC and ChrRCC

	Pseudoacinar	Fascicular	Reticular	Isolated
CCRCC				
Grades I and II	39		10	
Grades III and IV		35	17	
PRCC				
Grades I and II	1			7
Grades III and IV	1			1
ChrRCC				
Grades I and II	2		4	
Grades III and IV			4	

Ovidium Ferician et al. [32] studied the distribution patterns of blood vessels based on the smooth muscle cell distribution and vascular morphology. They defined four types of tumor blood vessels: reticular, diffuse, fascicular and trabecular. These authors found a fascicular pattern in the PRCC with mature vessels and thin, often collapsed, lumen. In contrast most of our cases presented an isolated pattern, with short, round or elongated vessels, with visible lumen, located between tumor cells with no interconnections.

Regarding CCRCC, the same authors described a fundamentally reticular pattern [32], whilst in our cases a pseudoacinar pattern predominated; and in ChrRCC they reported a diffuse pattern, whereas we observed a reticular pattern. Taking into account this wide variation in blood vessel patterns, it is clear that these tumors present a complex and heterogeneous vascularization which may impact prognosis.

We also studied possible differences between the measure of MVD with anti-CD31 and anti-CD34 immunohistochemistry. The $CD34^+$ MVD was significantly higher in CCRCC than in PCCR and ChrRCC ($p < 0.001$) which implies that tumor vessels in CCRCC are more differentiated, which may be an influencing factor in the higher local aggressiveness of this type of tumor, however, no statistically significant differences were in the other two tumor variants. The present results contradict the findings of Eberhard et al. [39]. Their study implied that compared with most of the common cancers, RCC possesses a vasculature with a significantly higher proportion of immature microvessels stained by CD31 in CCRCC. Nevertheless, we found that $CD34^+$ vessels better correlate with the ISUP grading system than $CD31^+$. It also indicates that when selecting a marker to assess renal vasculature, both immature and mature vessels under CD31 and CD34 markers are important and provide useful additional information.

Conclusions

Our study defines four vascular patterns in renal cell carcinomas, based on morphology and morphometric parameters: pseudoacinar, fascicular, reticular and isolated. These patterns seem to be significantly related with the ISUP tumor grade.

Analysis of both mature and immature vessels (CD34+ and CD31+) provides additional information when evaluating microvascular density.

Compliance with Ethical Standards

Conflict of Interest We declare no conflict of interest.

References

1. Zhang B, Ji H, Yan D, Liu S, Shi B (2014) Lack of association of microvessel density with prognosis of renal cell carcinoma: evidence from meta-analysis. Tumor Biol 35(3):2769–2776
2. Döme B, Hendrix MJC, Paku S, Tóvári J, Tímár J (2007) Alternative vascularization mechanisms in cancer. Am J Pathol 170(1):1–15
3. Srigley JR, Delahunt B (2009) Uncommon and recently described renal carcinomas. Mod Pathol 22(Suppl 2):S2–23
4. Murphy WM, Grignon DG, Perlman EJ (2004) Tumors of the kidney, bladder, and related urinary structures. American Registry of Pathology, Washington
5. Delahunt B, Eble JN, McCredie MR, Bethwaite PB, Stewart JH, Bilous AM (2001) Morphologic typing of papillary renal cell carcinoma: comparison of growth kinetics and patient survival in 66 cases. Hum Pathol 32:590–595
6. Storkel S, Eble JN, Adlakha K et al (1997) Classification of renal carcinoma. Cancer 80:987–989
7. Thoenes W, Storkel S, Rompelt HJ, Moll R, Baum HP, Werner S (1988) Chromophobe cell renal carcinoma and its variants. A report in 32 cases. J. Pathol 155:277–287
8. Hlatky L, Hahnfeldt P, Folkman J (2002) Clinical application of antiangiogenic therapy: microvessel density, what it does and doesn't tell us. J Nat Cancer Inst 94:883–893
9. Grizzi F, Colombo P, Barbieri B et al (2001) Microscopic analysis and significance of vascular architectural complexity in renal cell carcinoma. Clin Cancer Res 7:3305–3307
10. Weidner N, Semple JP, Welch WR, Folkman J (1991) Tumor angiogenesis and metastasis: correlation in invasive breast carcinoma. N Engl J Med 324:1–8
11. Grizzi F, Ceva-Grimaldi G, Dioguardi N (2001a) Fractal geometry: a useful tool for quantifying irregular lesions in human liver biopsy specimens. Ital J Anat Embryol 106:337–346
12. Kovacs G, Akhtar M, Beckwith BJ et al (1997) The Heidelberg classification of renal cell tumours. J Pathol 80:992–993
13. Ljungberg B, Bensalah K, Canfield S, Dabestani S, Hofmann F, Hora M, et al (20015). EAU Guidelines on Renal Cell Carcinoma 2014 Update. Eur Urol 67(5): 913–924
14. Delahunt B, Srigley JR, Montironi R, Egevad L (2014) Advances in renal neoplasia: recommendations from the 2012 International Society of Urological Pathology Consensus Conference. Urology 83(5):969–974
15. Poblet E, González-Palacios F, Jimenez FJ (1996) Different immunoreactivity of endotelial markers in well and poorly differentiated areas of angiosarcomas. Virchows Arch 428:217–221
16. Yilmazer D, Han U, Onal B (2007) A comparison of the vascular density of VEGF expression with microvascular density determined with CD34 and CD31 staining and conventional prognostic markers in renal cell carcinoma. Int Urol Nephrol 39:691–698
17. Meert AP, Paesmans M, Martin B, Delmotte P, Berghmans T, Verdebout JM, Lafitte JJ, Mascaux C, Sculier JP (2002) The role of microvessel density on the survival of patients with lung cancer: a systematic review of the literature with meta-analysis. Br J Cancer 87:694–701
18. Uzzan B, Nicolas P, Cucherat M, Perret GY (2004) Microvessel density as a prognostic factor in women with breast cancer: a systematic review of the literature and meta-analysis. Cancer Res 64: 2941–2955
19. Des Guetz G, Uzzan B, Nicolas P, Cucherat M, Morere JF, Benamouzig R, Breau JL, Perret GY (2006) Microvessel density and VEGF expression are prognostic factors in colorectal cancer. Meta-analysis of the literature. Br J Cancer 94:1823–1832
20. Ruiz-Saurí A, Valencia-Villa G, Romanenko A, Pérez J, García R, García H, Benavent J, Sancho-Tello M, Carda C, Llombart-Bosch A (2016) Influence of exposure to chronic persistent low-dose ionizing radiation on the tumor biology of clear-cell renal-cell carcinoma. An Immunohistochemical and morphometric study of angiogenesis and vascular related factors. Pathol Oncol Res 22(4):807–815
21. Joo HJ, Oh DK, Kim YS, Lee KB, Kim SJ (2004) Increased expression of caveolin-1 and microvessel density correlates with metastasis and poor prognosis in clear cell renal cell carcinoma. BJU Int 93:291–296
22. Nativ O, Sabo E, Reiss A, Wald M, Madjar S, Moskovitz B (1998) Clinical significance of tumor angiogenesis in patients with localized renal cell carcinoma. Urology 51:693–696
23. Yoshino S, Kato M, Okada K (1995) Prognostic significance of microvessel count in low stage renal cell carcinoma. Int J Urol 2: 156–160
24. MacLennan GT, Bostwick DG (1995) Microvessel density in renal cell carcinoma: lack of prognostic significance. Urology 46:27–30
25. Minardi D, Lucarini G, Mazzucchelli R, Milanese G, Natali D, Galosi AB, Montironi R, Biagini G, Muzzonigro G (2005) Prognostic role of Fuhrman grade and vascular endothelial growth factor in pT1a clear cell carcinoma in partial nephrectomy specimens. J Urol 174:1208–1212
26. Anastassiou G, Duensing S, Steinhoff G, Zorn U, Grosse J, Dallmann I, Kirchner H, Ganser A, Atzpodien J (1996) Platelet endothelial cell adhesion molecule-1 (PECAM-1): a potential prognostic marker involved in leukocyte infiltration of renal cell carcinoma. Oncology 53:127–132
27. Imao T, Egawa M, Takashima H, Koshida K, Namiki M (2004) Inverse correlation of microvessel density with metastasis and prognosis in renal cell carcinoma. Int J Urol 11:948–953
28. Rioux-Leclercq N, Epstein JI, Bansard JY, Turlin B, Patard JJ, Manunta A, Chan T, Ramee MP, Lobel B, Moulinoux JP (2001) Clinical significance of cell proliferation, microvessel density, and CD44 adhesion molecule expression in renal cell carcinoma. Hum Pathol 32:1209–1215
29. Sabo E, Boltenko A, Sova Y, Stein A, Kleinhaus S, Resnick MB (2001) Microscopic analysis and significance of vascular architectural complexity in renal cell carcinoma. Clin Cancer Res 7:533–537
30. Schraml P, Struckmann K, Hatz F, Sonnet S, Kully C, Gasser T, Sauter G, Mihatsch MJ, Moch H (2002) VHL mutations and their correlation with tumour cell proliferation, microvessel density, and patient prognosis in clear cell renal cell carcinoma. J Pathol 196: 186–193
31. Cheng S-H, Liu J-M, Liu Q-Y, Luo D-Y, Liao B-.H, Li H, Wang K-J (2014). Prognostic role of microvessel density in patients with

renal cell carcinoma: a meta-analysis. Int J Clin Exp Pathol 7(9): 5855–5863
32. Ferician O, Cimpean AM, Ceasu AM, Dema A, Raica M, Cumpanas A (2016) Heterogeneous vascular patterns in renal cell carcinomas. Pol J Pathol 67(1):46–53
33. Joshi S, Singh AR, Durden DL (2015) Pan-PI-3 kinase inhibitor SF 1126 shows antitumor and antiangiogenic activity in renal cell carcinoma. Cancer Chemother Pharmacol 75:595–608
34. Schirner M, Hoffmann J, Menrad A, Schneider MR (1998) Antiangiogenic chemotherapeutic agents: characterization in comparison to their tumor growth inhibition in human renal cell carcinoma models. Clin Cancer Res 4:1331–1336
35. Travnicek I, Branzovsky H, Kalusova K, Hess O, Holubec L, Pele KB, Ürge T, Hora M (2015) Tissue biomarkers in predicting response to sunitinib treatment of metastatic renal cell carcinoma. Anticancer Res 35:5661–5666
36. Porta C, Giglione P, Liguigli W, Paglino C (2015) Dovitinib (CHIR258, TKI258): structure, development and preclinical and clinical activity. Future Oncol 11:39–50
37. Okoń K, Kawa R (2008) Microvascular network in renal carcinomas. Quantitative and tissue microarray immunohistochemical study. Pol J Pathol 59:107–115
38. Tinini T, Rossi F, Claudio PP (2003) Molecular basis of angiogenesis and cancer. Oncogene 22:6549–6556
39. Eberhard A, Kahlert S, Goede V, Hemmerlein B, Plate KH, Augustin HG (2000) Heterogeneity of angiogenesis and blood vessel maturation in human tumors: implications for antiangiogenic tumor therapies. Cancer Res 60:1388–1393